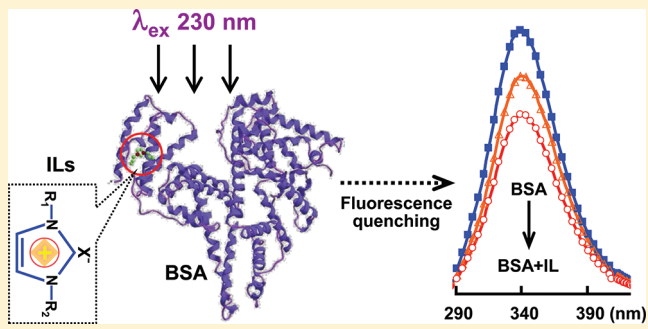


New Insight into Molecular Interactions of Imidazolium Ionic Liquids with Bovine Serum Albumin

Yang Shu, Menglin Liu, Shuai Chen, Xuwei Chen,* and Jianhua Wang*

Research Center for Analytical Sciences, Box 332, Northeastern University, Shenyang 110189, China

ABSTRACT: The interactions of imidazolium ionic liquids (ILs), i.e., dibutylimidazolium chloride, 1-butyl-3-methylimidazolium chloride, and 1-butyl-3-methylimidazolium nitrate, with bovine serum albumin (BSA) were studied by monitoring the spectral behaviors of IL–BSA aqueous systems. The intrinsic fluorescence of BSA at 340 nm excited at 230 nm is obviously quenched by these ILs due to complex dynamic collision and their quenching constants are at the order of 10^2 L mol^{-1} . However, no fluorescence quenching is observed within the same region when excited at 280 nm, which is widely used for probing protein conformations. Thermodynamic investigations reveal that the combination between ILs and BSA is entropy driven by predominantly hydrophobic and electrostatic interactions, leading to the unfolding of polypeptides within BSA. The influence of the ILs on the conformation of BSA follows a sequence of $\text{BmimNO}_3 > \text{BmimCl} \approx \text{BbimCl}$. Molecular docking shows that cationic imidazolium moieties of ILs enter the subdomains of protein and interact with the hydrophobic residues of domain III. An agreement between fluorescence spectroscopic investigations and molecular docking is reached. It is found that the fluorescence of BSA at $\lambda_{\text{ex}} 230 \text{ nm}$ arising from aromatic amino acids Trp and Tyr is almost as sensitive as that achieved at $\lambda_{\text{ex}} 280 \text{ nm}$ for elucidating the protein conformational changes, which provides a valid and new probe for the investigation of binding kinetics between molecules/ions and proteins.



1. INTRODUCTION

Ionic liquids (ILs) have shown great promise as a potential alternative to conventional volatile organic solvents due to their unique and attractive properties, e.g., negligible vapor pressure, nonflammability, high chemical/thermal stability, low toxicity, and favorable conductivity. They have been widely adopted in various fields including synthesis, separation, electrochemistry, catalysis, and chemical sensors.^{1–3}

ILs are gaining extensive attention in protein assays, because ILs not only provide a novel and highly efficient reaction medium but also serve as effective participants in various biological reaction processes. Usually, ILs are employed as neat solvents containing little or no water and emphasis is often placed on protein dynamics and structure due to their relationship to the protein activity, function, and stability.⁴ In addition, ILs may be used as cosolvents for water in biphasic systems. The two aqueous phase systems composed of ILs and phosphate are frequently applied for the separation of proteins.^{5,6} Investigations on the interactions between ILs and proteins in aqueous solutions are even more important than those in neat ILs phase.

The behaviors of proteins in IL phase have been frequently reported. The impact of various cation/anion pairings on the thermal stability of ribonuclease A in aqueous systems containing a range of imidazolium or bromide-based ILs were systematically elucidated by differential scanning calorimetry.⁷ Protein–IL interactions in aqueous media can be interpreted within a Hofmeister framework. Generally, the variations of anionic

moiety of ILs appear to have an even more obvious effect on protein properties than the cation variations do. The denaturation of cytochrome c and human serum albumin (HSA) in aqueous solution of water-miscible 1-butyl-3-methylimidazolium chloride is observed by small-angle neutron scattering and X-ray scattering.⁸ At IL concentration of 25% (v/v), the two proteins were found to largely retain their higher-order structures whereas both were highly denatured at 50% (v/v) of IL. It is reported that the fluorescent behavior of the acrylodan-labeled HSA in 1-butyl-3-methylimidazolium-based ionic liquid/water mixture is a function of temperature and water loading.⁹ The results revealed that the domain I of HSA appears to refold with a water load of above 30% (v/v). Up to now, the interactions between proteins and ionic liquids in aqueous media are not well understood and the underlying interpretations are still mostly speculative.

Bovine serum albumin (BSA) serves as a depot protein and as a transport protein for a variety of compounds. It is one of the most extensively studied of this group of proteins, particularly because of its structural homology with HSA.^{10,11} BSA consists of 583 amino acid residues and is made up of three homologous domains (I, II, and III). It contains 17 disulfide bridges that divide the protein into 9 loops (L1–L9).¹² It has two tryptophan (Trp) residues as intrinsic fluorophores, i.e., Trp134 in the first domain

Received: July 27, 2011

Revised: September 7, 2011

Published: September 15, 2011

and Trp212 in the second domain. Trp134 is located on the surface of the molecule, and Trp212 is found within a hydrophobic binding pocket of the protein. The intrinsic fluorescence of Trp facilitates the investigations of binding affinities between chemical molecules (ions) and BSA.^{13,14} It has been reported that Trp residues are buried in a hydrophobic microenvironment in the presence of 1-tetradecyl-3-methylimidazolium bromide, inducing BSA denaturation.¹⁵

In the present work, a comprehensive investigation is performed for the binding properties of imidazolium ionic liquids to BSA and thermodynamics for the binding reactions. Molecular docking is used to interpret the binding location of imidazolium ILs in BSA structure. We found for the first time that for investigating the interactions between ionic liquids and proteins, the fluorescence arising from Trp and Tyr with excitation at $\lambda_{\text{ex}} 230 \text{ nm}$ is almost as sensitive as that excited at $\lambda_{\text{ex}} 280 \text{ nm}$. This provides a new probe for elucidating protein–ion/molecule interactions.

2. EXPERIMENTAL SECTION

2.1. Chemicals. Bovine serum albumin (BSA, A3311) was purchased from Sigma (St. Louis, MO) and used without further purification. 1, 3-Dibutylimidazolium chloride (BbimCl), 1-butyl-3-methylimidazolium chloride (BmimCl), and 1-butyl-3-methylimidazolium nitrate (BmimNO₃) were purchased from Shanghai Cheng Jie Chemicals (Shanghai, China) and used as received. BSA and ILs were all prepared with 0.1 mol L⁻¹ Tris-HCl buffer (pH 7.4). Other chemicals employed are at least of analytical reagent grade. Deionized water of 18 MΩ cm⁻¹ is used throughout the experiments.

2.2. Spectral Measurements. UV–vis absorption spectra are recorded on a T6 UV–vis spectrophotometer (Purkinje General Instruments, Beijing, China) with a 1.0 cm quartz cuvette at room temperature (293 K). The spectra of BSA are achieved within Tris-HCl buffer and those of the IL–BSA systems are measured with IL aqueous solution as blank in order to eliminate the spectral inferences on the IL–BSA system from the ILs.

A F-7000 spectrophotometer (Hitachi, Japan) is used for the fluorescence measurement with a slit of 5 nm and a scan speed of 1200 nm min⁻¹. The scanning voltage of lamp is set to 500 V.

Circular dichroism (CD) spectra are obtained on a MOS-450 (Bio-Logic, France) automatic recording spectropolarimeter at 293 K in a wavelength range of 190–240 nm. The spectra are recorded with nitrogen protection by using 1 mm cell length with a scan rate of 200 nm min⁻¹. Each spectrum is accumulated at least twice, and the results are expressed as CD millidegrees or mean residue ellipticity (MRE) in deg cm² dmol⁻¹.

2.3. Molecular Docking. Molecular docking simulations are performed with the software package AutoDock Version 4.2 by applying the Lamarckian Genetic Algorithm.¹⁶ The crystal structures of proteins are from the Brookhaven Protein Data Bank (<http://www.rcsb.org/pdb>; entry codes: 1H9Z for HSA). The structure of HSA is assigned with Kollman-UTI charges in the Amber 4.0 force field. The geometry of IL is optimized using the Tripos force field with Gasteiger–Hückel charges. Both initial ligand molecules are in an arbitrary conformation orientation and position. Fifty independent docking runs are carried out for each ligand. The results are clustered according to the 1.0 Å root-mean-square deviation (rmsd) criteria. All torsion angles for each compound are considered flexible. The grid maps representing the proteins in the actual docking process are calculated with AutoGrid. The dimensions of the grids are thus

Scheme 1. Molecular Structures of (A) BbimCl, (B) BmimCl, and (C) BmimNO₃

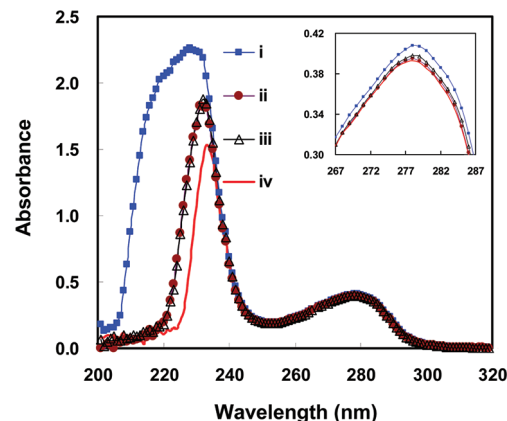
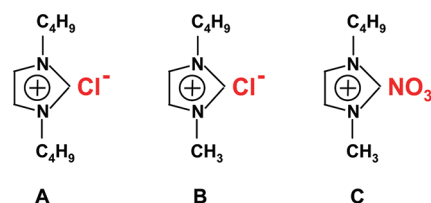


Figure 1. UV–vis spectra of BSA in the absence (i) and presence of ionic liquids. BbimCl–BSA (ii), BmimCl–BSA (iii), and BmimNO₃–BSA (iv). $C_{\text{IL}} = 1 \text{ mmol L}^{-1}$, $C_{\text{BSA}} = 10 \mu\text{mol L}^{-1}$, pH 7.4, and $T = 293 \text{ K}$.

60 Å × 60 Å × 60 Å, with a spacing of 0.375 Å between the grid points. After 100 runs, the most favorable docking model is selected according to the binding energy and the geometry matching.

3. RESULTS AND DISCUSSION

3.1. UV–vis Spectra. The molecular structures of three imidazolium ILs (BbimCl, BmimCl, and BmimNO₃) are illustrated in Scheme 1. The UV–vis spectra of BSA in the absence and presence of these ionic liquids are indicated in Figure 1.

Figure 1(i) shows two sorbet peaks from BSA at 226 and 278 nm, attributed to the $\pi-\pi^*$ transition of characteristic polypeptide backbone structure C=O¹⁷ and n– π^* transition of aromatic amino acids, i.e., tyrosine (Tyr), tryptophan (Trp), and phenylalanine (Phe).¹⁸

With the addition of ILs, an obvious decrease of the absorbance at 226 nm is observed along with a red-shift to ca. 238 nm (Figure 1(ii), (iii), (iv)). These spectral changes might arise from the disturbance of the microenvironment around the polypeptide caused by the binding of ILs with BSA. Usually, the amide moieties in the protein structure expose to a water environment would experience a low-energy $\pi-\pi^*$ transition under ultraviolet irradiation. In comparison with the electron cloud existing in the ground state, the π^* electron cloud has higher polarity because of the formation of an antibonding orbital between C and O in the excited state. As a polar solvent, a water molecule has a stronger ability to lower the energy of the π^* electron cloud rather than π electron cloud, although it lowers the energy levels of both states.¹⁷ When the microenvironment around the amide moieties of BSA is changed, i.e., the surrounding polar water molecules are

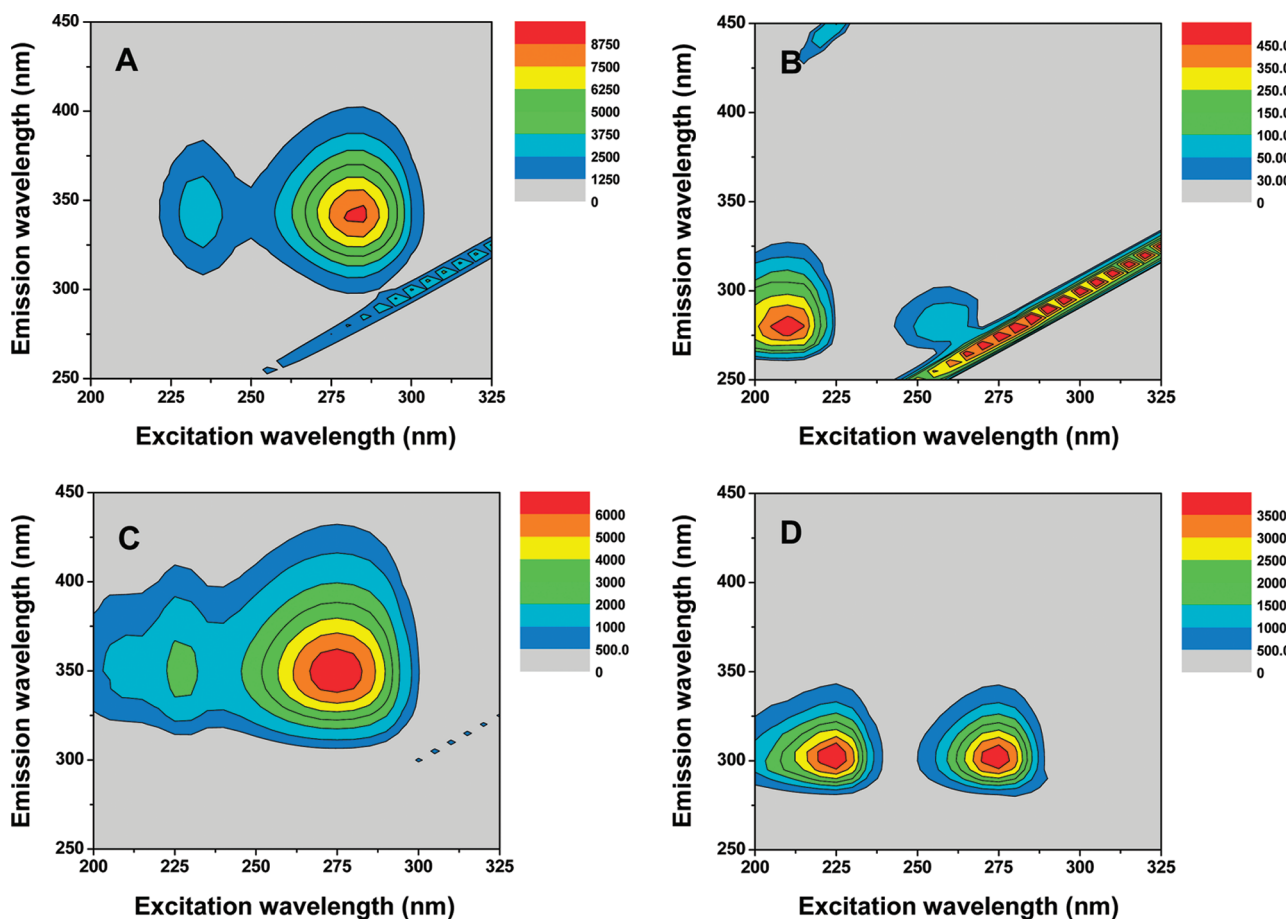


Figure 2. 3D fluorescent spectra of (A) BSA, (B) Phe, (C) Trp, and (D) Tyr aqueous solutions. $C_{\text{BSA}} = 10 \mu\text{mol L}^{-1}$, $C_{\text{Phe}} = C_{\text{Trp}} = C_{\text{Tyr}} = 100 \mu\text{mol L}^{-1}$, slit width of excitation and emission: 5 nm, voltage of lamp: 500 V.

displaced by the weak-polar IL moieties, a lower energy is required and the π^* transition would undergo a bathochromic shift and thus a hypochromic effect is observed.

Considering that the peak at 278 nm is related to the $n-\pi^*$ transition of aromatic amino acid, the subtle variation after addition of ILs further suggests that the microenvironment of the aromatic amino acid is changed due to the interactions between ILs and BSA.

The hydrophobicity of BBimCl is larger than that of the BmimCl due to the longer length of alkyl side chains in the cationic imidazolium moieties, however, almost identical UV-vis spectra are observed after introducing them into the reaction system (Figure 1 (ii) and (iii)). This suggests that the side chain of the imidazolium ring poses nearly no influence on the interactions between ILs and BSA.

On the contrary, although BmimCl and BmimNO₃ have an identical cationic imidazolium moieties, their interactions with BSA result in very different UV-vis spectra (Figure 1 (ii) and (iv)) due to the difference of anionic moiety in the ionic liquids. A significant decrease of the absorbance at 226 nm is observed for the BmimNO₃-BSA system with respect to that of the BmimCl-BSA system, in addition to a slight red shift of the absorption peak. These observations indicate that the interaction between BmimNO₃ and BSA is the strongest among the three tested ILs-BSA systems. It further illustrates that the anionic moieties of the imidazolium ILs play a very important role in the interactions of ionic liquids with proteins.

3.2. Fluorescence Spectra. Fluorescence quenching is the decrease of fluorescence quantum yield of a fluorophore induced by a variety of molecular interactions with quencher molecules. Fluorescence quenching is usually adopted to reveal the accessibility of the fluorophores to the quenchers.^{10,11} In the present case, the quenching of the intrinsic fluorescence of BSA by ILs is investigated to get information of the interactions between ILs and protein.

3D fluorescence spectrum of BSA. Figure 2 showed the three-dimensional (3D) fluorescence spectra of BSA and three monomeric aromatic amino acids, i.e., Phe, Trp and Tyr. It is obvious that two peaks are observed in the 3D fluorescence spectrum of BSA (Figure 2A), with maximum excitations/emissions at 230 nm/340 and 280 nm/340 nm, respectively. The 3D fluorescence spectra also shows that Phe is a weak fluorescent amino acid (Figure 2B), whereas distinct fluorescence peaks are recorded for Trp and Tyr within two excitation ranges, i.e., 225–230 and 270–275 nm for Trp (Figure 2C) and 220–225 and 270–275 nm for Tyr (Figure 2D). These observations illustrated that the fluorescent aromatic amino acids Trp and Tyr are the main contributors to the intrinsic fluorescence of BSA. The fluorescence peak at excitation/emission of 230 nm/340 nm in the 3D fluorescence spectrum has been demonstrated to be the characteristic fluorescence of polypeptide backbone structures,¹⁹ and thus the structure change of BSA tends to pose significant influence on the fluorescence.

Fluorescence Quenching. In the previous literature, imidazolium ILs are found to be fluorescent inducing by the imidazolium

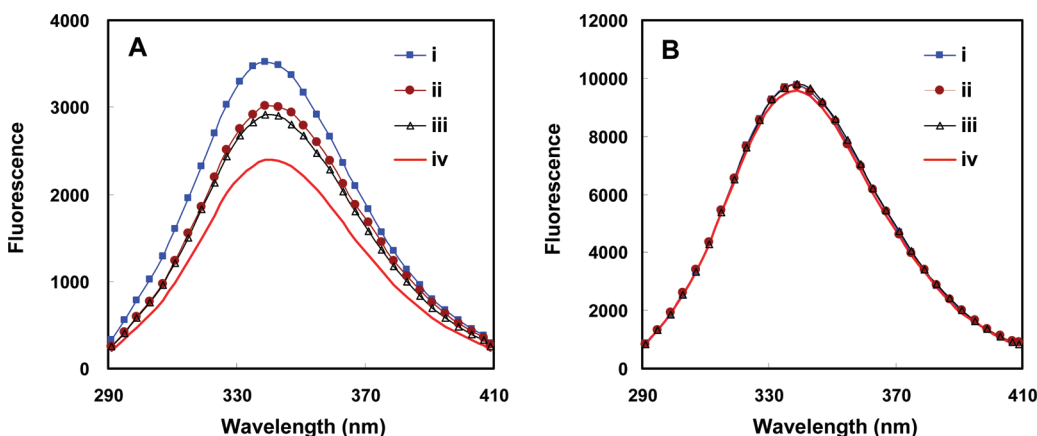


Figure 3. Fluorescence emission spectra of (i) BSA, (ii) BbimCl-BSA, (iii) BmimCl-BSA, and (iv) BmimNO₃-BSA. $C_{IL} = 1 \text{ mmol L}^{-1}$, $C_{BSA} = 10 \mu\text{mol L}^{-1}$, pH 7.4, and $T = 293 \text{ K}$.

moiety. However, their fluorescence efficiencies are generally very low, i.e., the measured fluorescence quantum yield of the neat imidazolium ILs, including BmimPF₆, BmimBF₄, and EmimBF₄, are between 0.005 and 0.02 when excited at 360 nm.²⁰ In the present investigations, the fluorescence intensity arises from the tested ILs at 340 nm, with excitation at 230 and 280 nm, respectively, is significantly lower than that of BSA obtained at the same conditions. On the other hand, though the imidazolium ILs have been demonstrated to have absorption in the UV region, the absorbance of BSA at 230 nm decreased with the addition of ILs, as showed in Figure 1, suggesting that the absorption of these ILs pose nearly no effect on the absorption of BSA. That is to say, the spectral interference from the ILs to the ILs-BSA interaction system is negligible.

Figure 3 showed the fluorescence spectra of BSA in the presence of ILs with excitation of 230 and 280 nm, respectively. It can be seen that obvious fluorescence quenching are observed by the addition of the three ILs when excited at 230 nm (Figure 3A) and a maximum quenching is obtained by BmimNO₃. On the other hand, however, virtually no fluorescence quenching is observed for the ionic liquids-BSA systems when excited at 280 nm (Figure 3B). The fluorescence quenching recorded in the present study agreed well with the changes observed in the UV-vis spectra. It suggested that the shorter wavelength excitation peaks provided clearer evidence for the interactions between ILs and BSA. Therefore, the ensuing investigations are conducted by choosing an excitation wavelength at 230 nm.

Fluorescence quenching might be dynamic resulting from collisions between the fluorophore and the quencher or static arising from the formation of a ground-state complex between the fluorophore and the quencher. In both cases, molecular contact is required between the fluorophore and the quencher for the fluorescence quenching.²¹

A quantitative estimation of the quenching is analyzed in terms of the quenching constant from the following Stern-Volmer equation.

$$\frac{F_0}{F} = 1 + K_{SV}[Q] = 1 + k_q \tau_0 [Q] \quad (1)$$

F_0 and F stand for the fluorescence intensities in the absence and presence of the quencher with a concentration of $[Q]$, $K_{SV} = k_q \tau_0$ is the Stern-Volmer quenching constant (for dynamic quenching), k_q is the bimolecular quenching constant, and τ_0 is

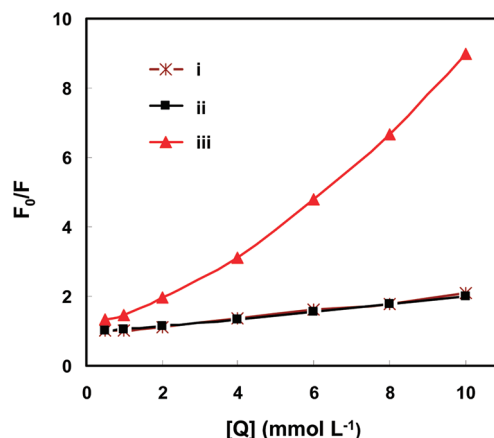


Figure 4. Stern-Volmer curves for fluorescence quenching of BSA in the systems of (i) BbimCl-BSA, (ii) BmimCl-BSA, and (iii) BmimNO₃-BSA. $C_{BSA} = 10 \mu\text{mol L}^{-1}$, pH 7.4, and $T = 293 \text{ K}$.

the lifetime of the fluorophore in the absence of the quencher. The quenching constant can be obtained from the slope of the Stern-Volmer plot of F_0/F versus $[Q]$.

As seen in Figure 4 (i) and (ii) that linear relationship is observed for F_0/F versus $[Q]$ for BbimCl-BSA and BmimCl-BSA systems when exciting at λ_{ex} 230 nm. The bimolecular quenching constants (k_q) for BbimCl-BSA and BmimCl-BSA systems, calculated from $K_{SV} = k_q \tau_0$ ($\tau_0 = 10^{-8} \text{ s}$), are $1.2 \times 10^{10} \text{ L mol}^{-1} \text{ s}^{-1}$ and $1.0 \times 10^{10} \text{ L mol}^{-1} \text{ s}^{-1}$, respectively. Considering both of the quenching constants are smaller than the largest possible bimolecular quenching constant of $2 \times 10^{10} \text{ L mol}^{-1} \text{ s}^{-1}$ in aqueous medium, the fluorescence quenching of BSA by BbimCl and BmimCl are most probably attributed to dynamic collision.

Figure 5 illustrates the Stern-Volmer curves of IL-BSA systems at different temperatures, and the K_{SV} values achieved from the Stern-Volmer equation are listed in Table 1. The increase of quenching constants for both the systems of BbimCl-BSA and BmimCl-BSA is clearly observed with the increase of temperature further demonstrated that the fluorescence quenching of BSA induced by the ionic liquids of BbimCl and BmimCl are attributed to dynamic quenching.

The Stern-Volmer plot of the BmimNO₃-BSA system in Figure 4c showed an upward curvature, indicating the possibility

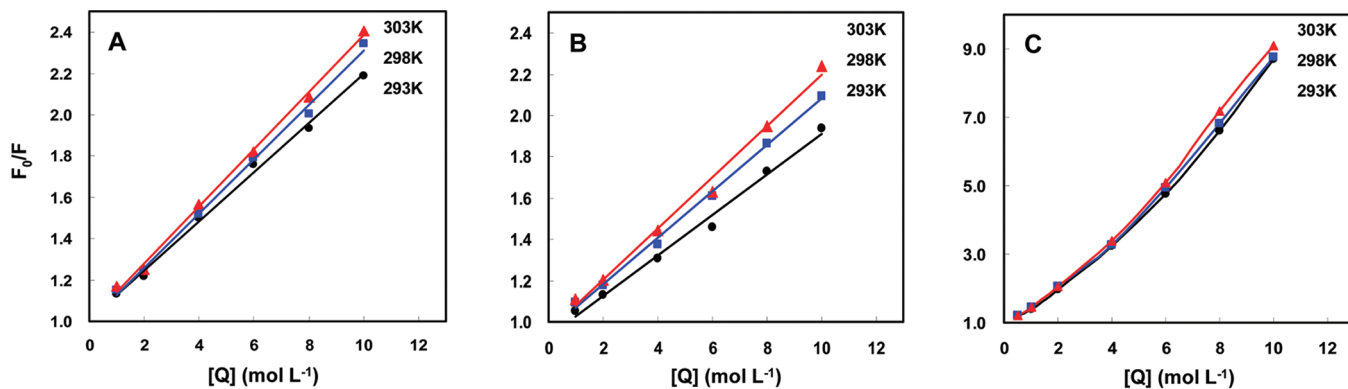


Figure 5. Stern–Volmer curves of fluorescence quenching of BSA in the systems of (A) BbimCl–BSA, (B) BmimCl–BSA, and (C) BmimNO₃–BSA at different temperatures. $C_{\text{BSA}} = 10 \mu\text{mol L}^{-1}$, $C_{\text{IL}} = 1 \text{ mmol L}^{-1}$, and pH 7.4.

Table 1. Stern–Volmer Quenching Constants for the IL–BSA Systems

		K_{SV} (L mol^{-1})	V	R^2	S.D.
BbimCl	293 K	117		0.9966	0.85
	298 K	129		0.9966	1.13
	303 K	136		0.9972	2.55
BmimCl	293 K	96		0.991	0.14
	298 K	111		0.9962	0.07
	303 K	122		0.9922	2.33
BmimNO ₃	293 K	429	51	0.9998	3.59
	298 K	439	44	0.9991	2.68
	303 K	468	41	0.9989	4.13

of a combined quenching process, e.g., static and dynamic quenching. The fluorescence data are analyzed by a modified Stern–Volmer equation as in the following:²²

$$\frac{F_0}{F} = 1 + K_{\text{SV}}[Q] \exp(V[Q]) \quad (2)$$

V is the static quenching constant, its value could be obtained from the modified Stern–Volmer equation by plotting $F_0/(F \exp(V[Q]))$ versus $[Q]$ by varying V until a linear plot is achieved. The K_{SV} could then be calculated from the slope. The values of V and K_{SV} at different temperatures (293, 298, and 303 K) are presented in Table 1. The larger values for K_{SV} than that for V suggests that the overall quenching is dominated by dynamic format, although a small contribution of static quenching is observed to the positive deviation of the Stern–Volmer plot.

Binding Parameters. When small molecules bind independently to a set of equivalent sites on a macromolecule, the equilibrium between the free and the bound molecules is given by the following equation:²³

$$\log \frac{F_0 - F}{F} = n \log K_A - n \log \frac{1}{[Q_t] - \frac{(F_0 - F)[P_t]}{F_0}} \quad (3)$$

F_0 and F are the fluorescence intensities before and after the addition of the quencher, K_A is the apparent binding constant to a set of sites, and n is the average number of binding sites per BSA. $[Q_t]$ and $[P_t]$ are the total quencher concentration and the total protein concentration, respectively. The intensity at 340 nm ($\lambda_{\text{ex}} = 230 \text{ nm}$) is used to calculate the binding constant.

Table 2. Apparent Binding Constants for the IL–BSA Systems

		K_A (L mol^{-1})	n	R^2	S.D.
BbimCl	293 K	123	0.9977	0.9935	1.36
	298 K	129	0.9603	0.9940	2.07
	303 K	137	0.9474	0.9895	2.78
BmimCl	293 K	95	1.2401	0.9987	1.01
	298 K	106	1.0841	0.9977	0.43
	303 K	116	1.0436	0.9959	2.59
BmimNO ₃	293 K	488	1.2697	0.9994	5.67
	298 K	519	1.2284	0.9988	4.14
	303 K	525	1.2541	0.9992	4.98

Table 3. Thermodynamic Parameters for the Ionic Liquid–BSA Interactions

		ΔG (kJ mol^{-1})	ΔH (kJ mol^{-1})	ΔS ($\text{J mol}^{-1} \text{K}^{-1}$)
BbimCl	293 K	-11.7		7.80
	298 K	-12.1		
	303 K	-12.4		
BmimCl	293 K	-11.1	15.0	89.1
	298 K	-11.5		
	303 K	-12.0		
BmimNO ₃	293 K	-15.1	5.52	70.4
	298 K	-15.5		
	303 K	-15.8		

The results for the three ionic liquids at different temperatures (293, 298, and 303 K) are given in Table 2. In general, the high-affinity binding constants between ligand-protein complexes locate in the range of 10^6 – 10^8 L mol^{-1} .²⁴ However, the obtained binding constants of the ionic liquid–BSA systems are very low (10^2 L mol^{-1}), which indicated a relatively weak interaction between the imidazolium ionic liquids and BSA.

Thermodynamic Parameters and the Nature of Binding Forces. The interaction forces involved in the binding of macro-biomolecules with small molecules usually include hydrogen bond formation, van der Waals, electrostatic and hydrophobic forces. By plotting the binding constants (K_A in Table 2) versus temperature according to the vant Hoff equation (eqs 4 and 5),

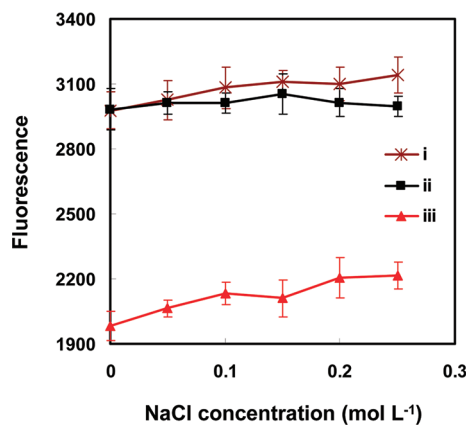


Figure 6. Effect of the concentration of NaCl on the fluorescence of the ionic liquid–BSA interaction systems. (i) BbimCl–BSA, (ii) BmimCl–BSA, and (iii) BmimNO₃–BSA. C_{IL} = 1 mmol L⁻¹ and C_{BSA} = 10 μmol L⁻¹.

the thermodynamic parameters are obtained from a linear vant Hoff plot as summarized in Table 3.

$$\ln K = -\frac{\Delta H}{TR} + \frac{\Delta S}{R} \quad (4)$$

$$\Delta G = \Delta H - T\Delta S \quad (5)$$

K is the equilibrium binding constant (L mol⁻¹), T is the temperature (K), and R is the gas constant (8.314 J mol⁻¹ K⁻¹).

The negative ΔG values indicate that the binding interactions between the three ionic liquids and BSA are spontaneous processes. On the other hand, the positive values for ΔH and ΔS suggest that hydrophobic forces and electrostatic attractions are the major driving forces for the ionic liquid–BSA binding interactions.²⁵

With an isoelectric point of 5.8, BSA is negatively charged in a Tris-HCl buffer of pH 7.4. Therefore, the electrostatic attraction between the ionic liquid cationic moieties and the negatively charged BSA facilitates the binding of ILs with BSA. Figure 6 shows the dependence of the fluorescence of the IL–BSA systems with the ionic strength. It is obvious that a slight increase of the fluorescence of the IL–BSA system is observed with the increase of NaCl concentration. This observation clearly indicates that the interactions between the ionic liquid moieties with BSA are weakened by salt effect which results in a decrease of the fluorescence quenching effect. These results well demonstrated that the binding of the ionic liquids with BSA is governed by electrostatic interactions.

3.3. BSA Conformational Investigations. Synchronous Fluorescence Spectra. Synchronous fluorescence screening is a useful technique to acquire information about the molecular environment in the vicinity of the chromophore molecules. The environment of the amino acid residues is evaluated by measuring the shift in the maximum emission wavelength corresponding to the changes of the polarity around the chromophore molecules. As referring to protein assays, the synchronous fluorescence spectra with $\Delta\lambda = 15$ and 60 nm are characteristics of Tyr and Trp residues, respectively.²⁶ To explore the structural change of BSA induced by the addition of ionic liquids, synchronous fluorescence spectra of BSA with various amounts of IL are recorded with $\Delta\lambda = 15$ and 60 nm, as illustrated in Figure 7. The results indicated that the presence of ILs leads to fluorescence quenching of BSA, while the characteristic emission wavelength

kept unchanged in any case. It is obvious that much more quenching is recorded when $\Delta\lambda$ of 60 nm is adopted. This suggests that the cationic imidazolium moieties of the ionic liquids are closer to the Trp residue than to the Tyr residue in the interaction system.

Circular Dichroism. The circular dichroism (CD) spectra of BSA in the absence and presence of IL are shown in Figure 8. It is clear that BSA exhibits two clear negative bands in the far-UV region at 208 and 222 nm which are characteristic of the α -helical structure of proteins, attributed to the n–π* transition for the peptide bond of α -helicity.²⁷ A quantitative estimation of the α -helix content of BSA and its complex (or additive) with ILs at different molar ratios are analyzed from the observed CD spectra. The CD results obtained are expressed in terms of mean residue ellipticity (MRE) in deg cm² dmol⁻¹ according to the following eq 6.

$$\text{MRE} = \frac{\text{observed CD}}{C_p n l 10} \quad (6)$$

C_p is the molar concentration of the protein, n is the number of amino acid residues of the target protein, which is 585 for BSA, and l is the path length in cm (0.1). The α -helical contents of both the free and the bound BSA are then calculated from the MRE values at 208 nm by using eq 7.

$$\alpha-\text{helix}(\%) = \frac{(-\text{MRE}_{208} - 4000)}{33000 - 4000} \times 100 \quad (7)$$

MRE₂₀₈ is the observed MRE value, 4000 is the MRE value of the β -form and random coil conformation, and 33000 is the MRE value of a pure α -helix. A significant decrease of the helical contents of the IL–BSA complex, e.g., from 41% to 29% for BbimCl–BSA (Figure 8), is observed with the increment of ILs concentration from 0.5 to 2 mmol L⁻¹. The reason might lie in the fact that the extended polypeptide structures of BSA caused by the binding of ILs led to the exposure of the hydrophobic cavities and the perturbation of the microstructures around the aromatic amino acid residues. The unfolding of BSA resulted in the exposure of more binding sites and the helical contents decreased dramatically.²⁸

An even more obvious decrease of the content of α -helicity of BmimNO₃–BSA is recorded, which is in accordance with the results of the UV–vis spectra and fluorescence spectra. The influence of the variations of anionic moiety of the ionic liquids on the protein properties had been demonstrated to be more prominent than that of the cationic moiety,^{29,30} this is well supported by the results of the addition of BmimCl, BmimNO₃, and KNO₃ into BSA solution, among which similar strong quenching effect were observed for BmimNO₃ and KNO₃. It is found that the number of hydrogen bonds formed between NO₃⁻ and protein is approximately twice of that formed between PF₆⁻ and protein.³¹ It seems that NO₃⁻ interacts strongly with the protein and enters the protein interior and therein disrupts the essential intraprotein hydrogen bonds, in particular in the α -helix regions.

3.4. Molecular Docking. The crystal structure of HSA is available online. The 3D structure of the crystalline HSA reveals the major regions of the ligand binding located in the hydrophobic cavities in the subdomains.³² Due to the structural homology between BSA and HSA, Autodock 4.2 is applied to examine the binding mode of IL in HSA. The optimum binding mode and binding site are given in Figure 9. 1,3-Dibutylimidazolium

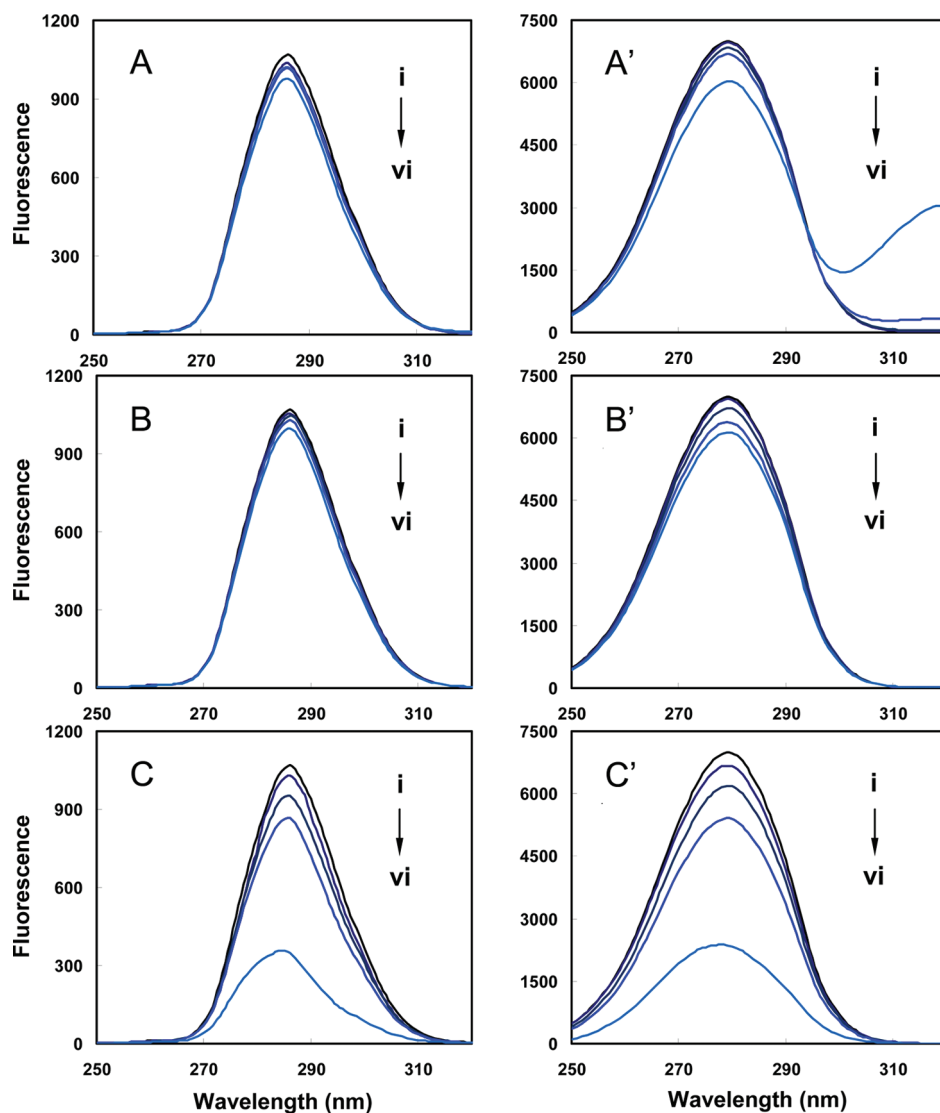


Figure 7. Synchronous fluorescence spectra of BSA in the presence of ionic liquids. (A) BbmimCl–BSA, $\Delta\lambda = 15$ nm, (A') BbmimCl–BSA, $\Delta\lambda = 60$ nm, (B) BmimCl–BSA, $\Delta\lambda = 15$ nm, (B') BmimCl–BSA, $\Delta\lambda = 60$ nm, (C) BmimNO₃–BSA, $\Delta\lambda = 15$ nm, and (C') BmimNO₃–BSA, $\Delta\lambda = 60$ nm. (i–vi): 0, 0.5, 1.0, 2.0, and 4.0 mmol L⁻¹ IL with 10 μ mol L⁻¹ BSA.

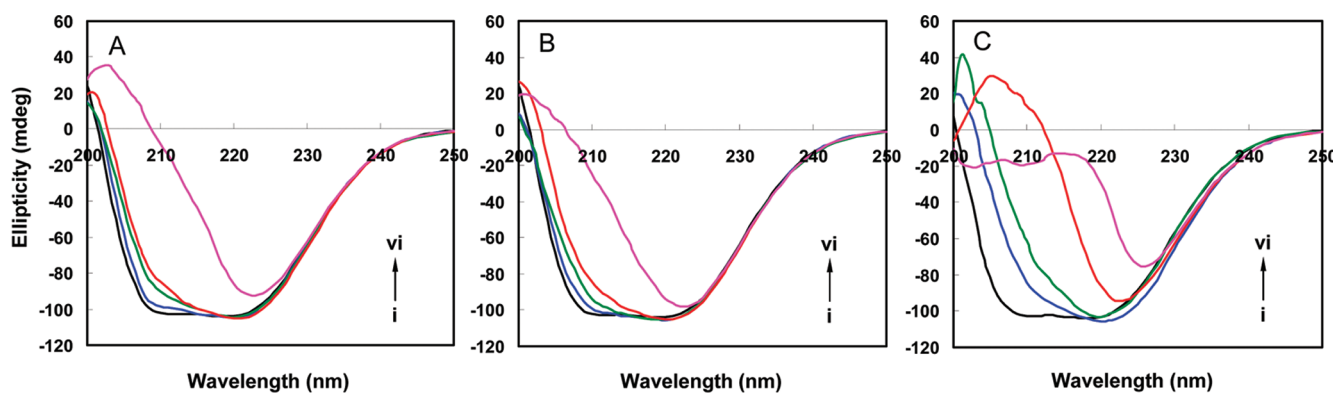


Figure 8. CD spectra of (A) BbmimCl–BSA, (B) BmimCl–BSA, and (C) BmimNO₃–BSA systems obtained in a 0.1 mol L⁻¹ Tris-HCl buffer of pH 7.4 at 293 K. (i–vi): 0, 0.5, 1.0, 2.0, and 4.0 mmol L⁻¹ of IL with 10 μ mol L⁻¹ BSA.

cation ($Bbmim^+$) is adjacent to the hydrophobic residues Phe502, Phe507, Phe509, Ala528, Leu532, Phe551, Leu575, Val576, and

Ser579 of domain III in HSA. 1-Butyl-3-methylimidazolium cation ($Bmim^+$) is similar to $Bbmim^+$ and surrounded by hydrophobic

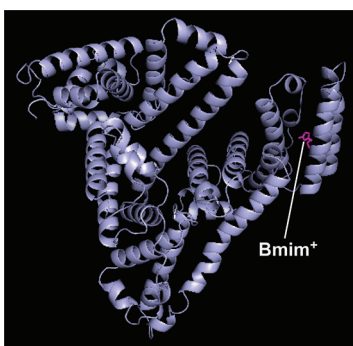


Figure 9. Molecular docking of imidazolium ionic liquid (BmimCl) and HSA.

residues Phe502, Phe507, Phe509, Val547, Phe551, Leu575, Val576, and Ser579. This suggests that hydrophobic force is the main interaction forces in the binding of imidazolium ILs to HSA, which is supported by the thermodynamic analysis. In addition, there are two charged amino acid residues, i.e., Lys536 and Gln580, thus the electrostatic interaction might also be involved in the binding of the ionic liquid to HSA. This agreed well with the thermodynamic analysis.

It is important to note that the Trp214 residue of HSA located in drug site 1 (subdomain IIA) is far away from the ionic liquid moiety. This finding provides a good structural basis to correlate the results with the absence of the fluorescence quenching data of BSA emission spectra in the presence of IL with $\lambda_{\text{ex}} = 280 \text{ nm}$.

The agreement between the results of molecular docking and those of fluorescence spectroscopy suggested that the fluorescence of protein excited at 230 nm (F230) is sensitive to protein conformation and F230 is thus provided a valid and convenient probe to determine the binding kinetics between molecules/ions and proteins.

4. CONCLUSIONS

An excitation wavelength of 230 nm is for the first time used to investigate the fluorescence quenching of BSA by imidazolium ionic liquids. The results suggested noncovalent attach of the ILs to BSA, far away from the fluorophore Trp212. The fluorescence intensity of BSA is quenched following a dynamic or static-dynamic combined quenching mechanism. By means of spectroscopy and molecular docking, we have discovered and interpreted the loss of secondary and tertiary structure of BSA induced by different amounts of ILs and concluded that the driving forces include hydrophobic and electrostatic interactions. For imidazolium ILs, anionic moiety variation seems to have even more obvious effect on protein properties than that of the cationic moiety. The present work elucidates the mechanism of imidazolium ionic liquids–BSA interactions. In addition, it creates a new fluorescent approach for the evaluation of ionic liquid-protein interactions with excitation at 230 nm.

AUTHOR INFORMATION

Corresponding Author

*E-mail: chenxuwei@mail.neu.edu.cn (X.-W.C.); jianhuajrz@mail.neu.edu.cn (J.-H.W.). Tel: +86 24 83688944. Fax: +86 24 83676698.

ACKNOWLEDGMENT

Financial supports from the Natural Science Foundation of China (No. 20805004, National Science Fund for Distinguished Young Scholars No. 20725517 and Major International Joint Research Project 20821120292), the Fundamental Research Funds for the Central Universities (N090405004, N090105001) and SRFDP program (200801451020) are highly appreciated.

REFERENCES

- (1) Liu, J. F.; Jonsson, J. A.; Jiang, G. B. Application of ionic liquids in analytical chemistry. *Trac-Trend. Anal. Chem.* **2005**, *24*, 20.
- (2) Anderson, J. L.; Armstrong, D. W.; Wei, G. T. Ionic liquids in analytical chemistry. *Anal. Chem.* **2006**, *78*, 2892.
- (3) Liu, R.; Liu, J. F.; Yin, Y. G.; Hu, X. L.; Jiang, G. B. Ionic liquids in sample preparation. *Anal. Bioanal. Chem.* **2009**, *393*, 871.
- (4) Moniruzzaman, M.; Nakashima, K.; Kamiya, N.; Goto, M. Recent advances of enzymatic reactions in ionic liquids. *Biochem. Eng. J.* **2010**, *48*, 295.
- (5) Pei, Y. C.; Wang, J. J.; Wu, K.; Xuan, X. P.; Lu, X. J. Ionic liquid-based aqueous two-phase extraction of selected proteins. *Sep. Purif. Technol.* **2009**, *64*, 288.
- (6) Du, Z.; Yu, Y. L.; Wang, J. H. Extraction of proteins from biological fluids by use of an ionic liquid/aqueous two-phase system. *Chem.—Eur. J.* **2007**, *13*, 2130.
- (7) Constantinescu, D.; Weingärtner, H.; Herrmann, C. Protein denaturation by ionic liquids and the Hofmeister series: a case study of aqueous solutions of ribonuclease A. *Angew. Chem., Int. Ed.* **2007**, *46*, 8887.
- (8) Baker, G. A.; Heller, W. T. Small-angle neutron scattering studies of model protein denaturation in aqueous solutions of the ionic liquid 1-butyl-3-methylimidazolium chloride. *Chem. Eng. J.* **2009**, *147*, 6.
- (9) Page, T. A.; Kraut, N. D.; Page, P. M.; Baker, G. A.; Bright, F. V. Dynamics of loop 1 of domain I in human serum albumin when dissolved in ionic liquids. *J. Phys. Chem. B* **2009**, *113*, 12825.
- (10) Bhattacharya, B.; Nakka, S.; Guruprasad, L.; Samanta, A. Interaction of bovine serum albumin with dipolar molecules: fluorescence and molecular docking studies. *J. Phys. Chem. B* **2009**, *113*, 2143.
- (11) Guharay, J.; Sengupta, B.; Sengupta, P. K. Protein-flavonol interaction: fluorescence spectroscopic study. *Proteins* **2001**, *43*, 75.
- (12) Jeyachandran, Y. L.; Mielezarski, E.; Rai, B.; Mielczarski, J. A. Quantitative and qualitative evaluation of adsorption/desorption of bovine serum albumin on hydrophilic and hydrophobic surfaces. *Langmuir* **2009**, *25*, 11614.
- (13) Papadopoulou, A.; Green, R. J.; Frazier, R. A. Interaction of flavonoids with bovine serum albumin: a fluorescence quenching study. *J. Agric. Food. Chem.* **2005**, *53*, 158.
- (14) McCarty, T. A.; Page, P. M.; Baker, G. A.; Bright, F. V. Behavior of acrylodan-labeled human serum albumin dissolved in ionic liquids. *Ind. Eng. Chem. Res.* **2008**, *47*, 560.
- (15) Geng, F.; Zheng, L. Q.; Yu, L.; Li, G. Z.; Tung, C. H. Interaction of bovine serum albumin and long-chain imidazolium ionic liquid measured by fluorescence spectra and surface tension. *Process. Biochem.* **2010**, *45*, 306.
- (16) Wang, Z. G.; Ling, B. P.; Zhang, R.; Liu, Y. J. Docking and molecular dynamics study on the inhibitory activity of coumarins on aldose reductase. *J. Phys. Chem. B* **2008**, *112*, 10033.
- (17) Zhao, X. C.; Liu, R. T.; Chi, Z. X.; Teng, Y.; Qin, P. F. New insights into the behavior of bovine serum albumin adsorbed onto carbon nanotubes: comprehensive spectroscopic studies. *J. Phys. Chem. B* **2010**, *114*, S625.
- (18) Glazer, A. N.; Smith, E. L. Studies on the ultraviolet difference spectra of proteins and polypeptides. *J. Biol. Chem.* **1961**, *236*, 2942.
- (19) Sandhya, B.; Hegde, A. H.; Kalanur, S. S.; Katrahalli, U.; Seetharamappa, J. Interaction of triprolidine hydrochloride with serum albumins: Thermodynamic and binding characteristics, and influence of site probes. *J. Pharm. Biomed. Anal.* **2011**, *54*, 1180.

- (20) Mandal, P. K.; Paul, A.; Samanta, A. Excitation wavelength dependent fluorescence behavior of the room temperature ionic liquids and dissolved dipolar solutes. *J. Photochem. Photobiol. A* **2006**, *182*, 113.
- (21) Ojha, B.; Das, G. The interaction of 5-(alkoxy)naphthalen-1-amine with bovine serum albumin and its effect on the conformation of protein. *J. Phys. Chem. B* **2010**, *114*, 3979.
- (22) Mandal, P.; Ganguly, T. Fluorescence spectroscopic characterization of the interaction of human adult hemoglobin and two isatins, 1-methylisatin and 1-phenylisatin: a comparative study. *J. Phys. Chem. B* **2009**, *113*, 14904.
- (23) Wang, Y. Q.; Zhang, H. M.; Zhang, G. C.; Liu, S. X.; Zhou, Q. H.; Fei, Z. H.; Liu, Z. T. Studies of the interaction between paraquat and bovine hemoglobin. *Int. J. Biol. Macromol.* **2007**, *41*, 243.
- (24) Mandeville, J. S.; Froehlich, E.; Tajmir-Riahi, H. A. Study of curcumin and genistein interactions with human serum albumin. *J. Pharm. Biomed. Anal.* **2009**, *49*, 468.
- (25) Lia, D. J.; Jia, B. M.; Jin, J. Spectrophotometric studies on the binding of Vitamin C to lysozyme and bovine liver catalase. *J. Lumin.* **2008**, *128*, 1399.
- (26) Antonov, Y. A.; Wolf, B. A. Calorimetric and structural investigation of the interaction between bovine serum albumin and high molecular weight dextran in water. *Biomacromolecules* **2005**, *6*, 2980.
- (27) Sahoo, B. K.; Ghosh, K. S.; Dasgupta, S. Molecular interactions of isoxazolcurcumin with human serum albumin: spectroscopic and molecular modeling studies. *Biopolymers* **2008**, *91*, 108.
- (28) Rafati, A. A.; Bordbar, A. K.; Gharibi, H. The interactions of a homologous series of cationic surfactants with bovine serum albumin (BSA) studied using surfactant membrane selective electrodes. *B. Chem. Soc. Jpn.* **2004**, *77*, 1111.
- (29) Micaelo, N. M.; Baptista, A. M.; Soares, C. M. Parametrization of 1-butyl-3-methylimidazolium hexafluorophosphate/nitrate ionic liquid for the GROMOS Force Field. *J. Phys. Chem. B* **2006**, *110*, 14444.
- (30) Lau, R. M.; Sorgedrager, M. J.; Carrea, G.; Rantwijk, F.; Secundob, F.; Sheldon, R. A. Dissolution of candida antarctica lipase B in ionic liquids: effects on structure and activity. *Green Chem.* **2004**, *6*, 483.
- (31) Micaelo, N. M.; Soares, C. M. Protein structure and dynamics in ionic liquids. Insights from molecular dynamics simulation studies. *J. Phys. Chem. B* **2008**, *112*, 2566.
- (32) Abou-Zied, O. K.; Al-Shihhi, O. I. K. Characterization of sub-domain IIA binding site of human serum albumin in its native, unfolded, and refolded states using small molecular probes. *J. Am. Chem. Soc.* **2008**, *130*, 10793.